



OPEN

## MiR-196a-5p hinders vascular smooth muscle cell proliferation and vascular remodeling via repressing BACH1 expression

Ying Tong<sup>1,2,3</sup>, Dan-Dan Wang<sup>1,3</sup>, Yan-Li Zhang<sup>1</sup>, Shuai He<sup>1</sup>, Dan Chen<sup>1</sup>, Ya-Xian Wu<sup>1</sup> & Qing-Feng Pang<sup>1</sup>✉

Hyperproliferation of vascular smooth muscle cells (VSMCs) is a driver of hypertensive vascular remodeling. This study aimed to uncover the mechanism of BTB and CNC homology 1 (BACH1) and microRNAs (miRNAs) in VSMC growth and hypertensive vascular remodeling. With the help of TargetScan, miRWalk, miRDB, and miRTarBase online database, we identified that BACH1 might be targeted by miR-196a-5p, and overexpressed in VSMCs and aortic tissues from spontaneously hypertensive rats (SHRs). Gain- and loss-of-function experiments demonstrated that miR-196a-5p suppressed VSMC proliferation, oxidative stress and hypertensive vascular remodeling. Double luciferase reporter gene assay and functional verification showed that miR-196a-5p cracked down the transcription and translation of BACH1 in both Wistar Kyoto rats (WKYs) and SHRs. Silencing BACH1 mimicked the actions of miR-196a-5p overexpression on attenuating the proliferation and oxidative damage of VSMCs derived from SHRs. Importantly, miR-196a-5p overexpression and BACH1 knockdown cooperatively inhibited VSMC proliferation and oxidative stress in SHRs. Furthermore, miR-196a-5p, if knocked down in SHRs, aggravated hypertension, upregulated BACH1 and promoted VSMC proliferation, all contributing to vascular remodeling. Taken together, targeting miR-196a-5p to downregulate BACH1 may be a promising strategy for retarding VSMC proliferation and hypertensive vascular remodeling.

**Keywords** MiR-196a-5p, BACH1, Hypertension, Vascular remodeling, Oxidative stress

Hypertension, a multifactorial disease, precedes multiple cardiovascular disorders<sup>1–4</sup>. Vascular remodeling, a pathological benchmark of several cardiovascular ailments<sup>5</sup>, mainly manifest hyperproliferation of vascular smooth muscle cells (VSMCs), particularly in hypertension and atherosclerosis<sup>6,7</sup>. Thus, VSMCs have long been recognized as a target in the prevention and treatment of hypertension.

Noncoding RNAs, such as microRNA (miRNAs), are highly expressed in VSMCs exerting specific roles in VSMC phenotype switching, proliferation and migration, all of which are critical characteristics of hypertensive vascular remodeling<sup>8</sup>. miRNAs can induce translation repression or mRNA degradation by binding to the 3'-untranslated regions (3'-UTRs) of a target mRNA sequence<sup>9</sup>. The potentiality of miRNAs in countering hypertensive and cardiovascular remodeling has been extensively studied in patient cohorts and animal models<sup>10</sup>. New effective miRNA-based strategies in the diagnosis, prevention and treatment of hypertensive vascular remodeling are needed.

BTB and CNC homology 1 (BACH1), a stress-responsive transcriptional factor, can suppress the activity of cytoprotective factors<sup>11</sup>. For example, BACH1 deletion can activate myocardial expression of heme-oxygenase (HO)-1, reduce myocardial cell death in mice with ischemia/reperfusion injury, and alleviate cardiovascular oxidative damage<sup>11</sup>. Depletion of BACH1 protects the heart from pressure overload in mice<sup>11</sup>. VSMC-specific loss of BACH1 inhibits the transformation and proliferation of VSMCs, highlighting a crucial role of BACH1 in VSMC phenotypic transition and vascular homeostasis<sup>12</sup>. BACH1 deletion or knockdown attenuates atherosclerosis by suppressing endothelial cell inflammation<sup>13,14</sup>. BACH1 expression was upregulated in small arteries and VSMCs

<sup>1</sup>Department of Pathophysiology, Wuxi School of Medicine, Jiangnan University, 1800 Lihu Avenue, Binhu District, Wuxi 214122, Jiangsu Province, China. <sup>2</sup>Department of Pathophysiology, Nanjing Medical University, Nanjing 211166, Jiangsu, China. <sup>3</sup>These authors contributed equally: Ying Tong and Dan-Dan Wang. ✉email: qfpang@jiangnan.edu.cn

from spontaneously hypertensive rats (SHRs)<sup>15</sup>. Likewise, the expression of cytoprotective HO-1 diminishes in aged hypertensive mice, whereas its putative regulator BACH1 is upregulated<sup>16</sup>. These findings suggest a fundamental role of BACH1 in hypertensive vascular remodeling. However, this role and associated mechanisms remain to be fully elucidated. Here, we screened miRNAs that regulate BACH1, and explored the performance of miR-196a-5p/BACH1 axis in hypertensive vascular remodeling.

## Results

### Identification of miRNA targeting BACH1

BACH1, a well-known oxidative stress-responsive transcription factor, is related to oxidative damage of cardiovascular system<sup>11,17,18</sup>, and is critically linked to cardiovascular disorders, including hypertension<sup>12</sup>. Potential miRNAs that regulated BACH1 were explored using TargetScan, miRWalk, miRTarBase, and miRDB databases. Overall, 823 miRNAs, 2045 miRNAs, 144 miRNAs, and 187 miRNAs were found to regulate BACH1 in TargetScan, miRWalk, miRTarBase, and miRDB databases, respectively (Fig. 1a). Venn diagrams visualized 30 overlapping miRNAs (Fig. 1a, right panel). The conserved sites for miRNA families broadly conserved among vertebrates are shown in (Fig. 1b). According to the TargetScan database, four miRNAs with higher prediction scores were selected, including let-7g-5p, miR-30a-5p, miR-92b-3p, and miR-196a-5p (Fig. 1c). We then detected the mRNA levels of let-7g-5p, miR-30a-5p, miR-92b-3p, and miR-196a-5p in artery tissues of WKYs and SHRs. The mRNA level of miR-92b-3p was higher, while those of let-7g-5p and miR-196a-5p were lower in SHR aortic tissues when compared with controls (Fig. 1d). Interestingly, the decrease in miR-196a-5p expression was more pronounced in SHR-derived aortic tissues (Fig. 1d). Further, we used dual-luciferase reporter gene assay to determine the interaction between miR-196a-5p and BACH1. The TargetScan analysis revealed that BACH1 had a miR-196a-5p binding site at the 3'-untranslated region (3'-UTR). Meanwhile, the luciferase activity of wild-type BACH1 reported gene was inhibited by co-transfection of miR-196a-5p mimics, while the luciferase activity of BACH1-mutant reported gene was not changed by miR-196a-5p mimics, indicating that miR-196a-5p overexpression directly repressed the transcription of BACH1 in VSMCs (Fig. 1e). In summary, miR-196a-5p may participate in hypertensive vascular remodeling by targeting BACH1.

### Influences of miR-196a-5p on VSMC proliferation of WKYs and SHRs

Aberrant proliferation of VSMCs is a hallmark of vascular remodeling related diseases, including hypertension<sup>1,5</sup>. We then assessed whether miR-196a-5p can be manipulated to regulate the growth of VSMCs from WKYs and SHRs. The effectiveness of the transfection of the miR-196a-5p mimic and the knockdown of miR-196a-5p was confirmed by the changes of miR-196a-5p levels in VSMCs (Fig. 2a, c). The growth of VSMCs from SHRs was more pronounced than that from WKYs, but was inhibited by overexpression of miR-196a-5p, as evidenced by CCK-8 and EdU assays (Fig. 2b). Meanwhile, silencing miR-196a-5p not only induced the proliferation of WKY VSMCs, but also potentiated the proliferation of SHR VSMCs (Fig. 2d).

### Influences of miR-196a-5p on VSMC oxidative stress in WKYs and SHRs

Oxidative stress acts to initiate the phenotypic transformation of VSMCs and subsequent VSMC proliferation, apoptosis and migration in various vascular diseases, including hypertensive vascular remodeling<sup>19,20</sup>. We determined the role of miR-196a-5p in the production of ROS in VSMCs from WKYs or SHRs. ROS fluorescence was more intense in SHR VSMCs, but reduced after ectopic miR-196a-5p expression that showed no effect on WKY VSMCs (Fig. 3a). The performance of miR-196a-5p was also confirmed by the activity of NAD(P)H oxidase (Fig. 3b), along with the protein levels of NOX-2 and NOX-4 expression, two isoforms of NAD(P)H oxidase as primary resources of ROS in cardiovascular cells<sup>21,22</sup>. Both NOX2 and NOX4 protein expression in VSMCs was increased in the SHR. The miR-196a-5p mimic inhibited protein expression of NOX2 rather than NOX4 (Fig. 3c). In contrast, deficiency of miR-196a-5p further increased oxidative stress in SHR VSMCs (Fig. 3d–f).

### Influences of miR-196a-5p on BACH1 expression in VSMCs from WKYs and SHRs

Similar to the results in vivo, the expression of miR-196a-5p was obviously diminished at the mRNA level in SHR-derived VSMCs (Fig. 4a). Conversely, the mRNA and protein levels of BACH1 were largely lifted up in SHR VSMCs, when compared with those in WKY VSMCs, and were then markedly reversed by BACH1 knockdown (Fig. 4b). In addition, miR-196a-5p mimics transfection reduced the expression of BACH1 in both SHR and WKY VSMCs at mRNA and protein levels (Fig. 4c). Deletion of miR-196a-5p exhibited opposite Influences (Fig. 4d).

### Influences of BACH1 knockdown on VSMC proliferation and oxidative stress in WKYs and SHRs

Similar to what we observed in VSMCs transfected with miR-196a-5p mimics, loss of BACH1 prevented the aberrant proliferation of VSMCs in SHR (Fig. 5a–b). Moreover, silencing BACH1 and upregulating miR-196a-5p collectively curbed the proliferation of VSMCs from SHR (Fig. 5c–d). Meanwhile, BACH1 knockdown attenuated the formation of ROS and NADPH oxidase activation in SHR VSMCs (Fig. 6a–d). Consistently, BACH1 downregulation and miR-196a-5p upregulation imparted inhibitory influences on ROS generation and NOX2, but not on NOX4 in SHR VSMCs (Fig. 6e–h).

### Influences of miR-196a-5p knockdown on blood pressure and BACH1 expression

The blood pressure of the tail artery measured weekly by using a noninvasive computerized tailcuff system (NIBP, ADInstruments, Sydney, New South Wales, Australia). MiR-196a-5p knockdown had no significant effect on blood pressure in WKY, but aggravated hypertension at two weeks in the SHRs. (Fig. 7a). The miR-196a-5p levels fell in both the aortic and mesenteric artery (MA) tissues of WKYs and SHRs, reaffirming the efficacy of

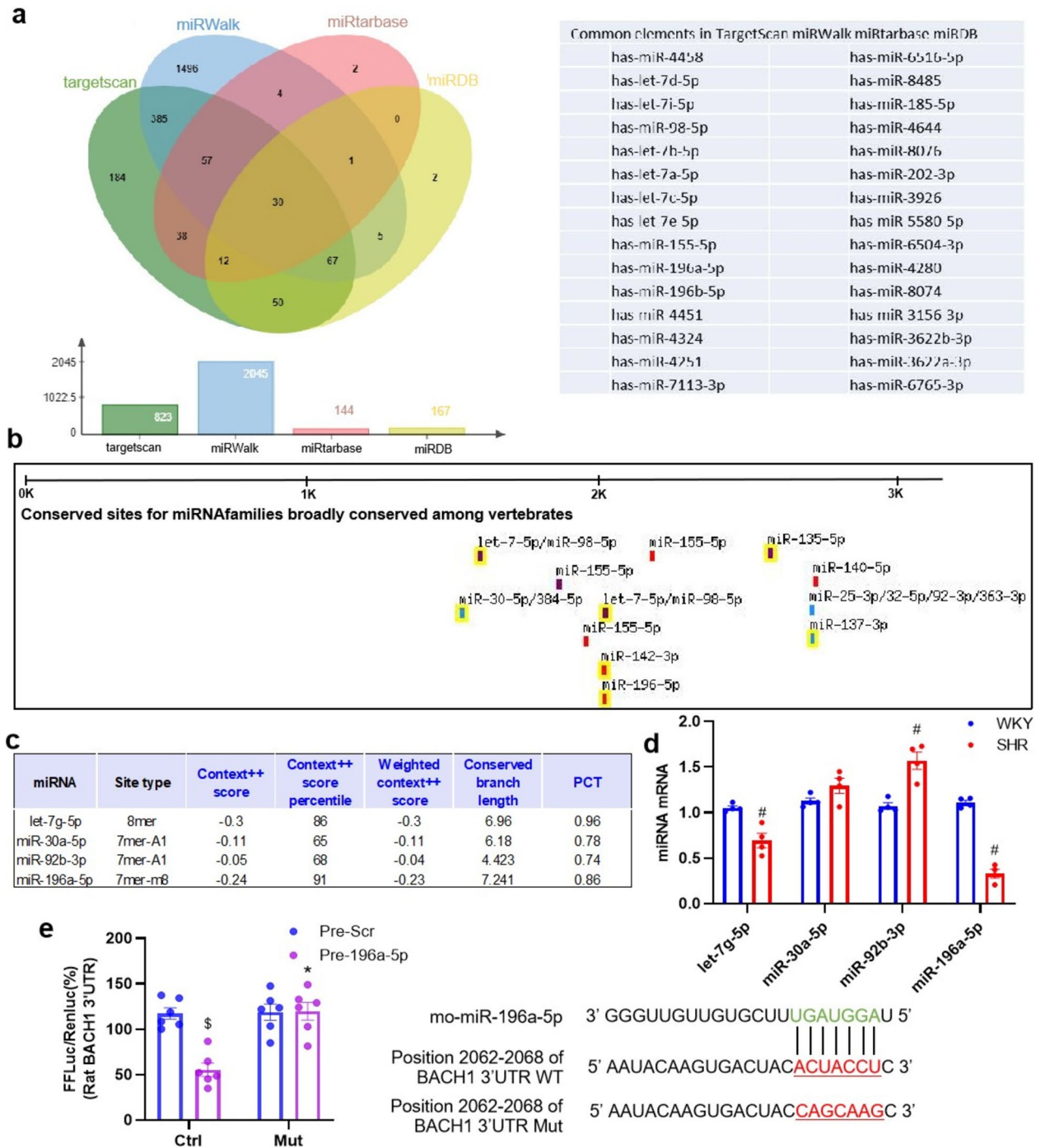


**Figure 1.** Identification of BACH1-targeting miR-196a-5p from miRNAs differentially expressed in the VSMCs of WKYs and SHRs. (a) Overlapping miRNAs in TargetScan, miRWalk, miRtarbase and miRDB. (b) Online prediction for BACH1 by TargetScanHuman. (c) Scores of prediction. (d) miRNA levels. (e) Prediction of the binding site of miRNA by TargetScanHuman. In the dual luciferase reporter assay, BACH1 was targeted by miR-196a-5p in VSMCs of WKY. FFLuc, Firefly luciferase; RenLuc, Renilla luciferase; WT, wild type; Mut, mutant type. Values were denoted as mean ± SEM. #  $p < 0.05$  vs WKY; \*  $p < 0.05$  vs Ctrl; §  $p < 0.05$  vs Pre-Scr.  $n = 4-6$ .

miR-196a-5p knockdown (Fig. 7b). miR-196a-5p knockdown increased BACH1 mRNA levels in the aortic and MA tissues of SHRs, compared with those of WKYs (Fig. 7c). Immunohistochemical analysis further confirmed that miR-196a-5p knockdown promoted BACH1 expression (Fig. 7d-e).

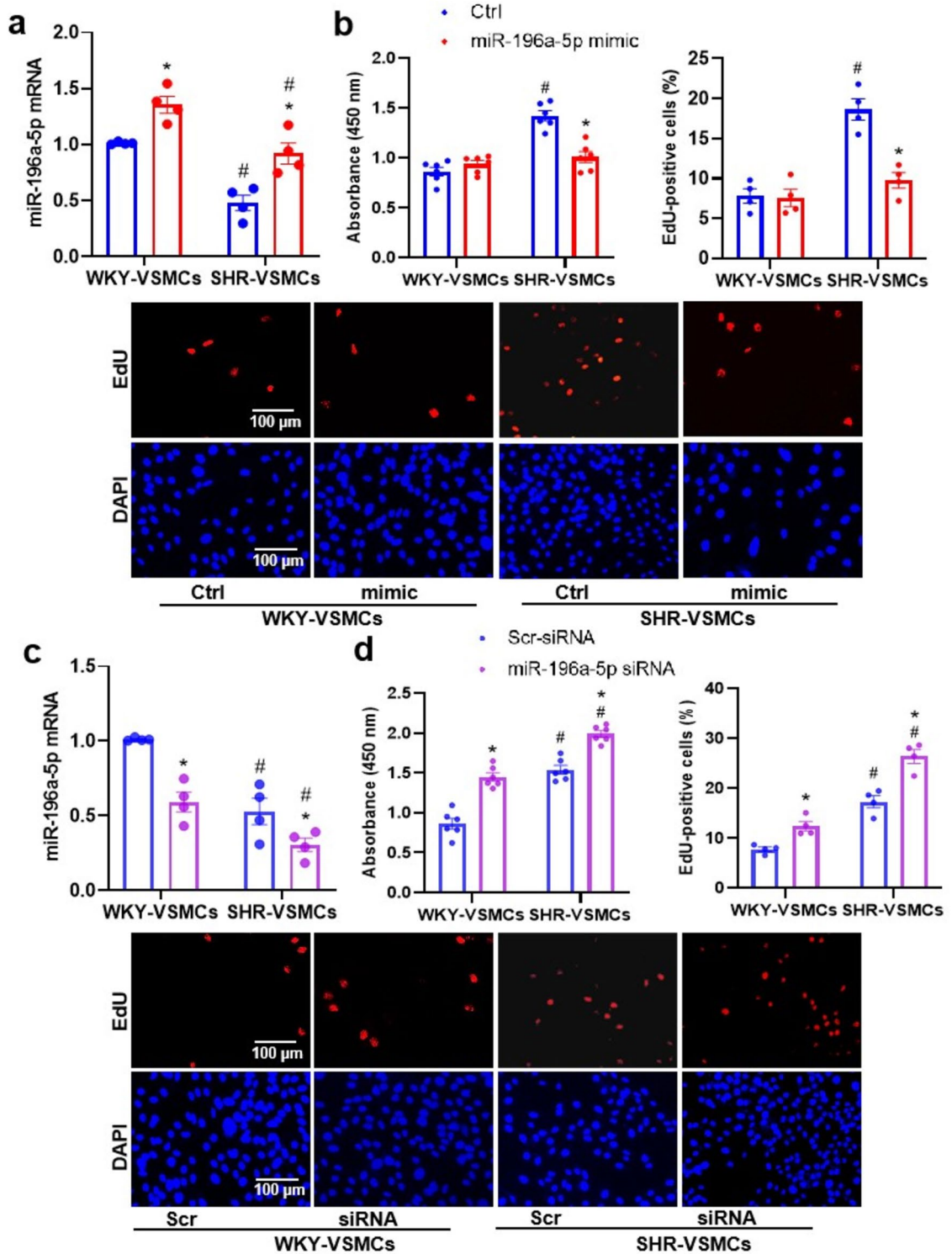


**Figure 2.** Influences of miR-196a-5p on VSMC proliferation in WKYs and SHRs. VSMC growth was assessed with CCK-8 and EdU assays. **(a, c)** miR-196a-5p levels in VSMCs. **(b)** Influences of miR-196a-5p mimics on VSMC proliferation. At 24 h after normal control (Ctrl, 50 nmol/L) or miR-196a-5p mimics (50 nmol/L) treatment. **(d)** Influences of miR-196a-5p siRNA on VSMC growth. At 48 h after control lentivirus (Scr-siRNA, 40 MOI) or miR-196a-5p siRNA (40 MOI) treatment. Values were denoted as mean  $\pm$  SEM. \*  $P < 0.05$  vs Ctrl. #  $P < 0.05$  vs WKY.  $n = 4-6$ .

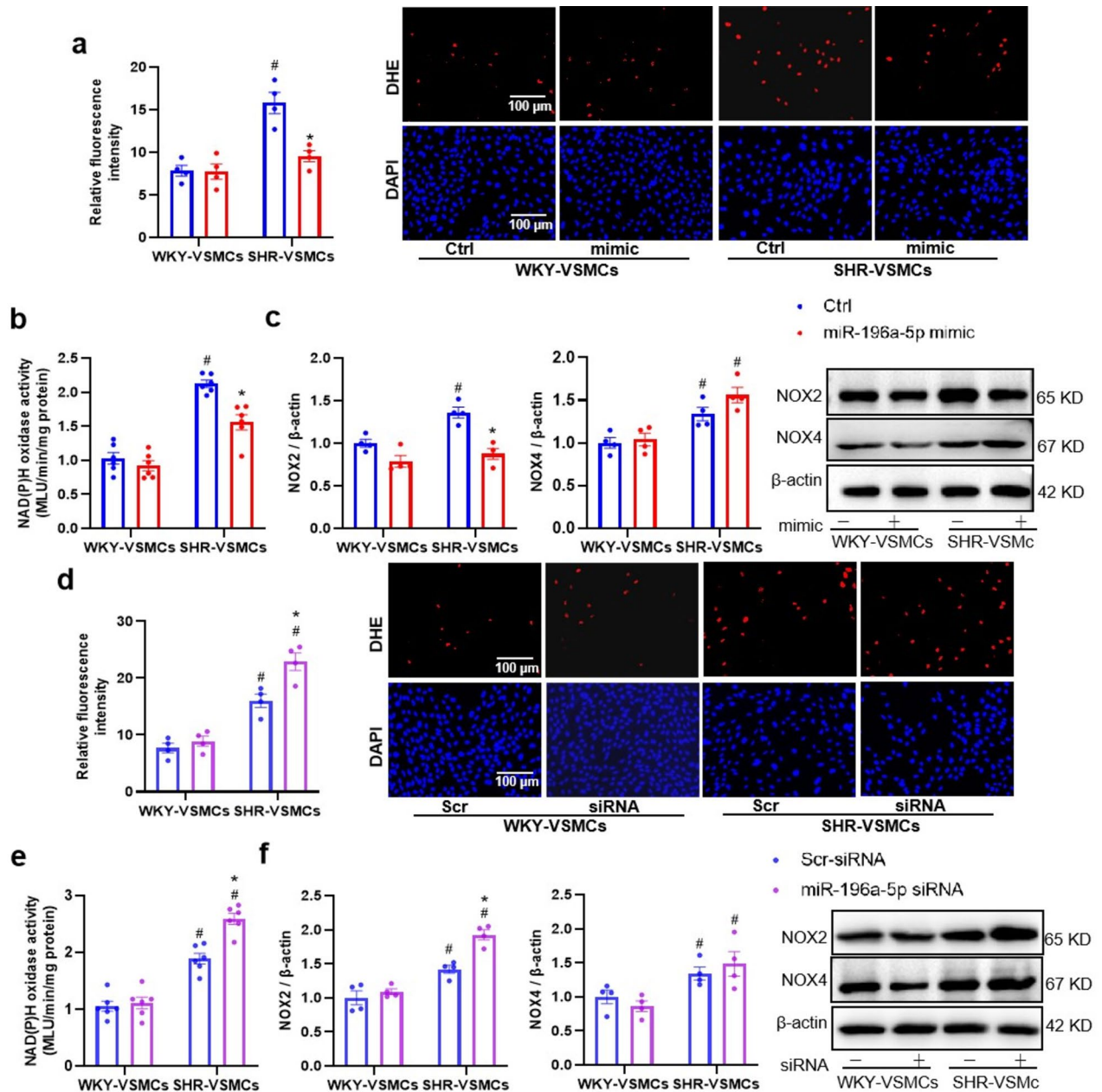


**Figure 3.** Influences of the miR-196a-5p on oxidative stress in VSMCs from WKYs and SHRs. After a 24-h treatment with normal control (Ctrl, 50 nmol/L), or miR-196a-5p mimics (50 nmol/L). After a 48-h treatment with control lentivirus (Scr-siRNA, 40 MOI) or miR-196a-5p siRNA (40 MOI). (**a, d**) ROS production assessed by red DHE fluorescence, and cell nuclei were stained blue with DAPI. (**b, e**) NAD(P)H oxidase activity. (**c, f**) NOX2 and NOX4 protein levels. Values were denoted as mean  $\pm$  SEM. \*  $p < 0.05$  vs Ctrl; #  $p < 0.05$  vs WKY.  $n = 4-6$ .

### Influences of miR-196a-5p knockdown on PCNA expression and vascular remodeling

MiR-196a-5p knockdown promoted the PCNA expression in the aortic tissues of SHRs (Fig. 8a–b). Masson's staining demonstrated larger media thickness, media thickness/lumen diameter ratio, and media cross-sectional area in the aortas and MA tissues of SHRs after miR-196a-5p knockdown (Fig. 8c–d), and the enlarged images of masson's staining in MA were provided in Supplement Figure S1. Taken together, miR-196a-5p attenuated vascular smooth muscle proliferation, vascular remodeling, and hypertension in SHRs.

### Discussion

Abnormal vascular remodeling elevates peripheral resistance and subsequent development of hypertension<sup>23,24</sup>. VSMCs may be targeted to treat vascular remodeling and associated hypertension<sup>25</sup>. Emerging evidences showed that miRNAs are used as biomarkers or therapeutic targets for several disease<sup>1,26,27</sup>, and the dysregulation of miRNAs is related to the pathogenesis of oxidative stress<sup>28,29</sup> and vascular disease<sup>30,31</sup>. Our previous researches

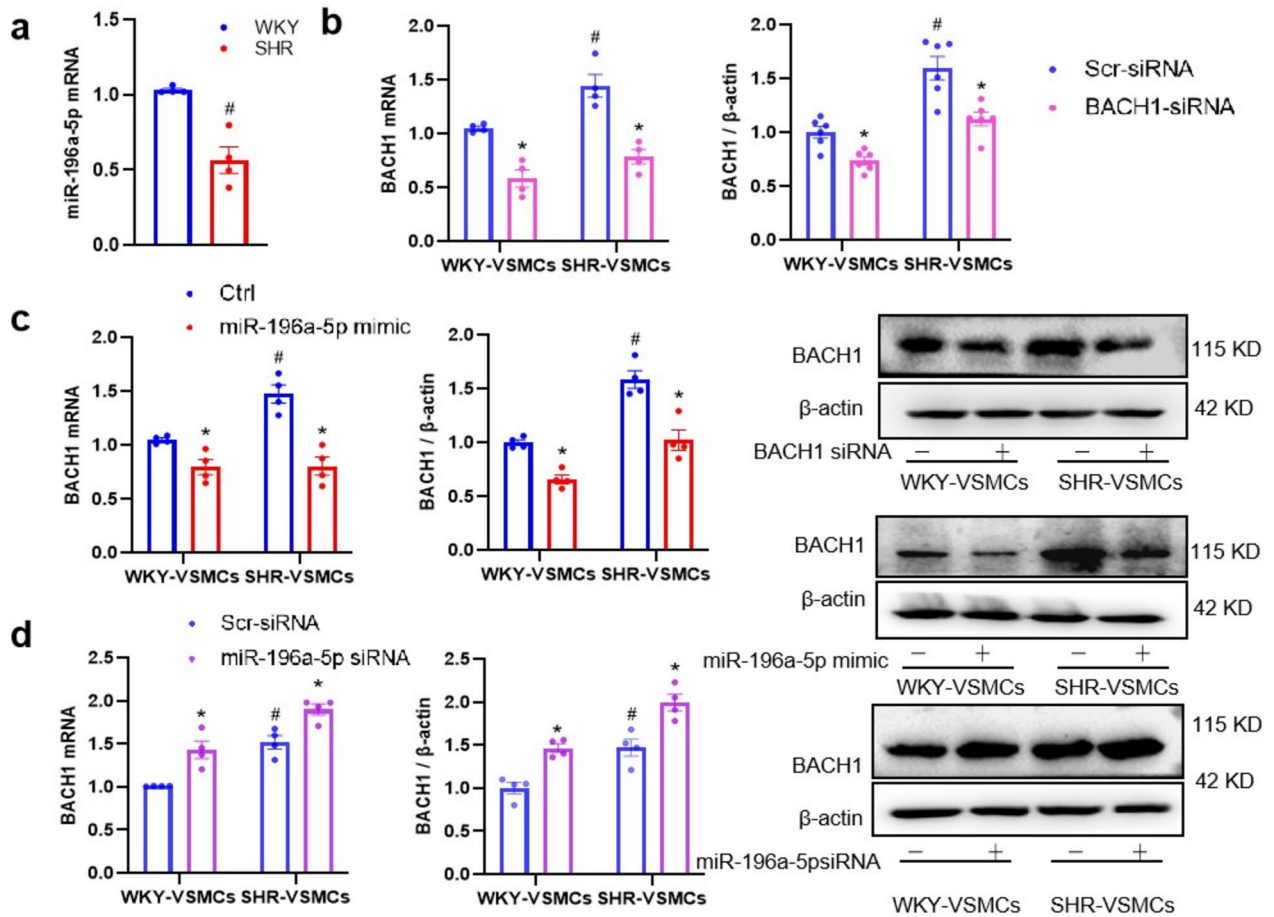


**Figure 4.** Influences of miR-196a-5p on BACH1 expression in VSMCs. **(a)** miR-196a-5p expressions in WKY and SHR VSMCs. **(b)** BACH1 mRNA and protein levels. After a 48-h treatment with control lentivirus (Scr-siRNA, 80 MOI) or BACH1-siRNA (80 MOI). **(c)** Influences of miR-196a-5p mimics on BACH1 mRNA and protein levels in VSMCs. At 24 h after negative control (Ctrl, 50 nmol/L) or miR-196a-5p mimics (50 nmol/L) treatment. **(d)** Influences of miR-196a-5p knockdown on BACH1 mRNA and protein levels in VSMCs. At 48 h after control lentivirus (Scr-siRNA, 40 MOI) or miR-196a-5p siRNA (40 MOI) treatment. Values were denoted as mean  $\pm$  SEM. <sup>\*</sup>  $p < 0.05$  vs Scr or Ctrl. <sup>#</sup>  $P < 0.05$  vs WKY.  $n = 4$ .

have found that miR-135a-5p, miR-31-5p and miR-155-5p are related to VSMC proliferation and migration<sup>32–34</sup>. MiR196a-5p is associated with cardiovascular diseases, but its role in hypertension is still unclear<sup>35,36</sup>. In this study, we found that under a hypertensive state, miR-196a-5p attenuated VSMC proliferation, oxidative stress and vascular remodeling by inhibiting the expression of BACH1. High expression of miR-196a-5p suppress the growth of VSMCs in SHRs. We provide robust evidence that miR-196a-5p might be exploited to cope with hypertensive vascular remodeling via repressing BACH1 transcription.

BACH1 can rein cellular responses to oxidative stress<sup>37</sup>. BACH1 also develops a negative association with Nrf2, a transcriptional factor that helps to maintain intracellular oxidation homeostasis<sup>38,39</sup>. BACH1 deficiency brings beneficial outcomes in many disorders<sup>40</sup>, including hypertensive diseases<sup>16</sup>. BACH1 regulates the expression of a battery of genes involved in oxidative stress and inflammatory responses<sup>41</sup>, two driving forces for the development of hypertensive vascular remodeling<sup>20</sup>. Elevated expression of BACH1 is observed in the vasculature from SHRs<sup>15</sup>. miRNAs- and BACH1-derived therapies may open a new window to prevent or treat hypertensive vascular remodeling. Here, we screened candidate miRNAs that may regulate BACH1 using TargetScan, miR-Walk, miRDB, and miTarBase online databases, and found that miR-196a-5p could directly bind to BACH1 mRNA (3'-UTR). The present study showed that BACH1 was targeted by miR-196a-5p in VSMCs. In view of the direct binding of miR-196a-5p with BACH1 and the obvious downregulation of miR-196a-5p in SHR VSMCs, we will further explore the contribution of miR-196a-5p to the biology of VSMCs in the context of hypertension.

In the present study, sustained miR-196a-5p expression attenuated the proliferation of VSMCs from SHRs, while miR-196a-5p ablation made SHR VSMCs more migrative, implying that miR-196a-5p can suppress VSMC migration and hypertensive vascular remodeling by restraining BACH1. Accordingly, loss of BACH1 attenuated the proliferation and oxidative damage of SHRs' VSMCs. By contrast, overexpression of BACH1 led to abnormal VSMC proliferation and oxidative burst. Collectively, the miR-196a-5p/BACH1 axis may be exploited to design new protective interventions for vascular remodeling in hypertension.

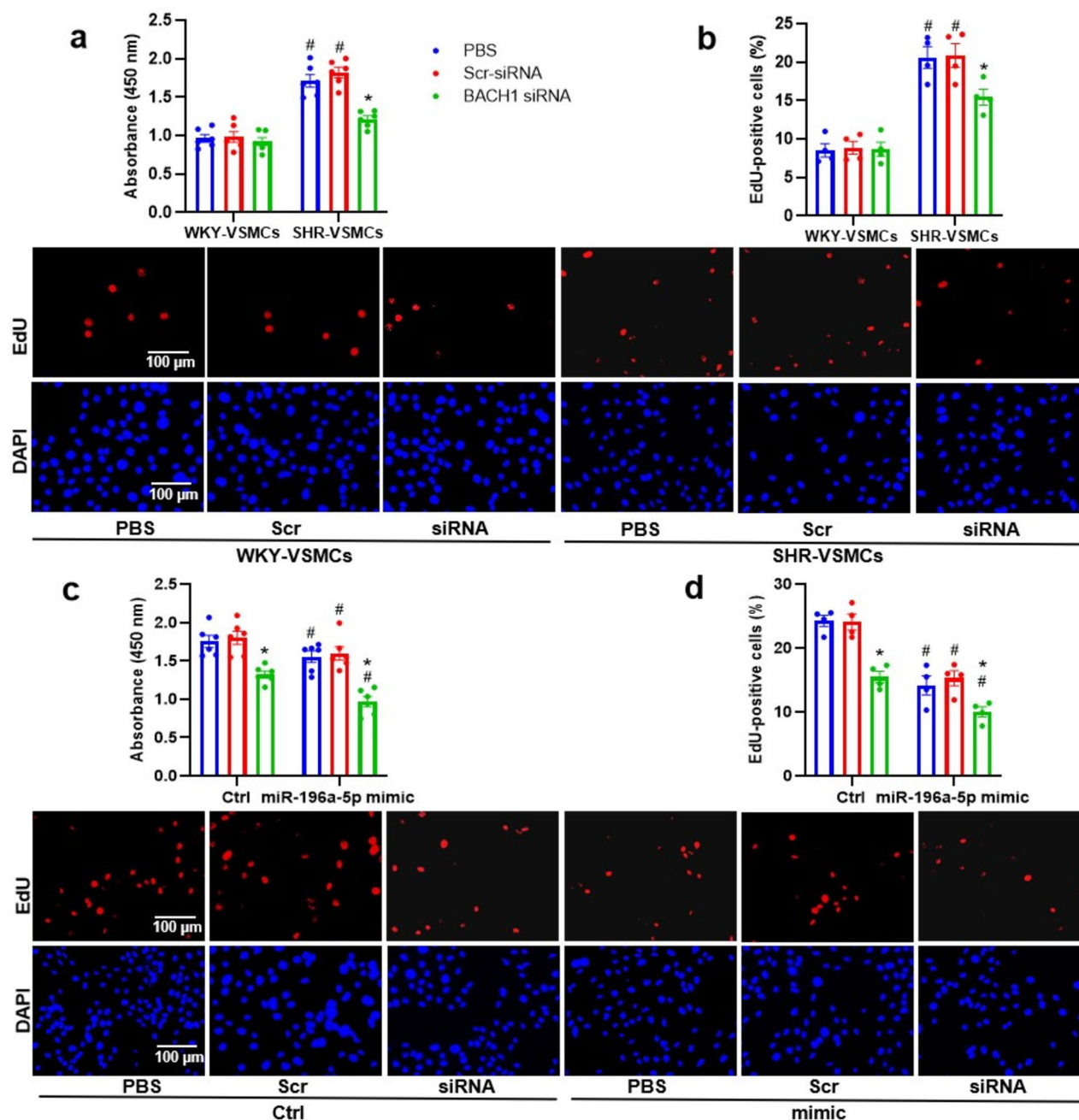


**Figure 5.** Influences of BACH1 knockdown on VSMC proliferation. VSMC proliferation was evaluated with CCK-8 and EdU incorporation assays. (**a**, **b**) Influences of BACH1-siRNA on VSMC proliferation. At 48 h after PBS, control lentivirus (Scr-siRNA, 80 MOI) or BACH1-siRNA (80 MOI) treatment. (**c**, **d**) Influences of BACH1-siRNA on miR-196a-5p mimic-induced VSMC proliferation in SHRs. SHR-VSMCs were treated for 48 h with PBS, control lentivirus (Scr-siRNA, 80 MOI) or BACH1-siRNA (80 MOI), followed by normal control (Ctrl, 50 nmol/L) or miR-196a-5p mimics (50 nmol/L) for 24 h. Values were denoted as mean  $\pm$  SEM. \*  $p < 0.05$  vs PBS; #  $p < 0.05$  vs WKY or Ctrl.  $n = 4-6$ .

## Conclusions

Collectively, miR-196a-5p protects against hypertension-induced VSMC oxidative stress, growth and vascular remodeling by suppressing the expression of BACH1. The miR-196a-5p/BACH1 axis is critically implicated in the proliferation of VSMCs under a hypertensive state, and may be employed to halt hypertensive vascular remodeling.

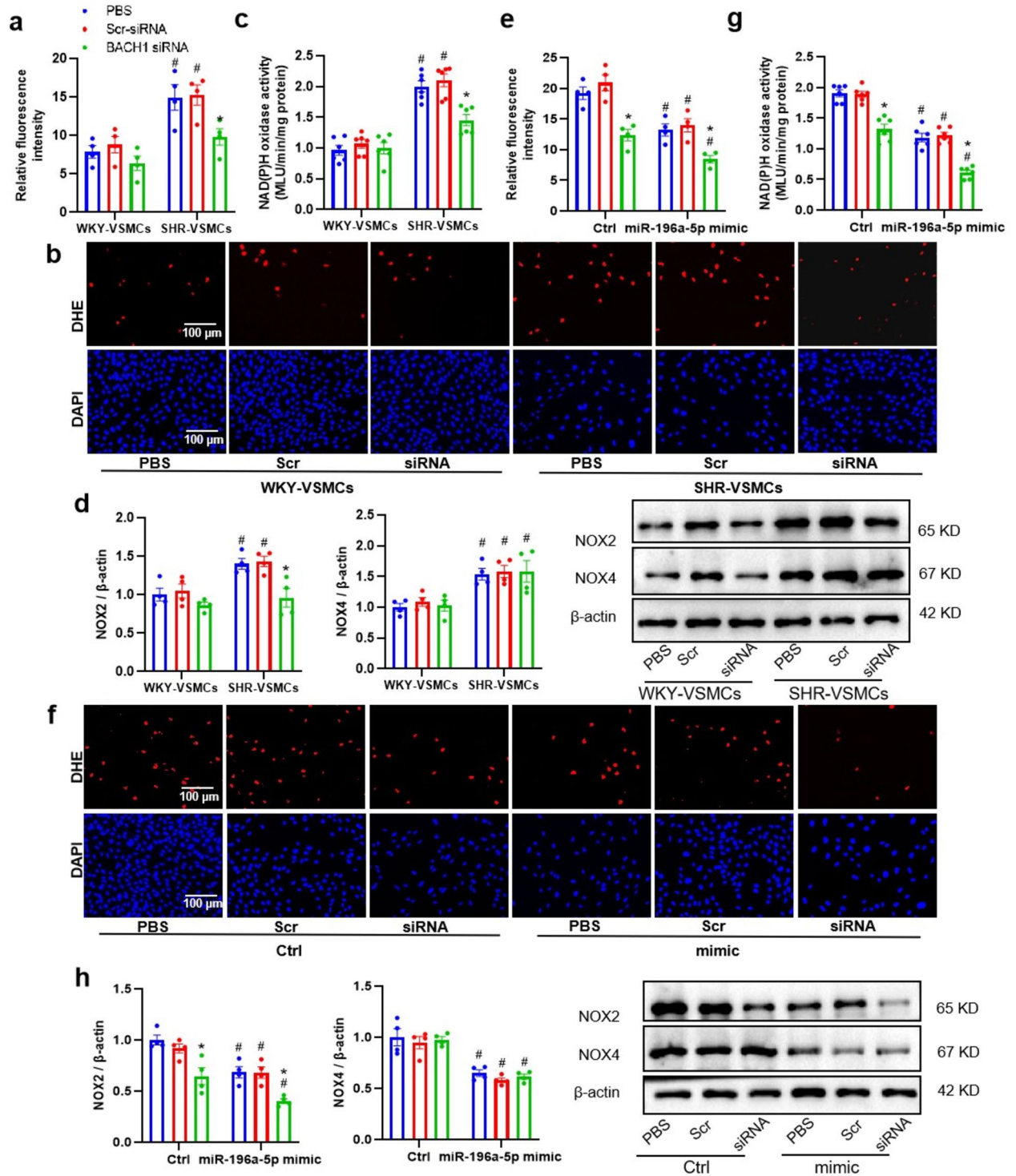


**Figure 6.** Influences of BACH1 knockdown on oxidative stress in VSMCs from WKY and SHRs. After a 48-h of treatment with PBS, control lentivirus (Scr-siRNA, 80 MOI) or BACH1-siRNA (80 MOI). Influences of BACH1-siRNA on miR-196a-5p mimic-induced oxidative stress in VSMCs of SHRs. SHR-VSMCs were treated with PBS, control lentivirus (Scr-siRNA, 80 MOI) or BACH1-siRNA (80 MOI) for 48 h, followed by normal control (Ctrl, 50 nmol/L) or miR-196a-5p mimics (50 nmol/L) for 24 h. (a, b, e, f) ROS production was detected by red DHE fluorescence, and cell nuclei were stained blue with DAPI. (c, g) NAD(P)H oxidase activity. (d, h) NOX2 and NOX4 protein expression. Values were denoted as mean  $\pm$  SEM. \*  $p < 0.05$  vs. PBS; #  $p < 0.05$  vs. WKY or Ctrl.  $n = 4-6$ .



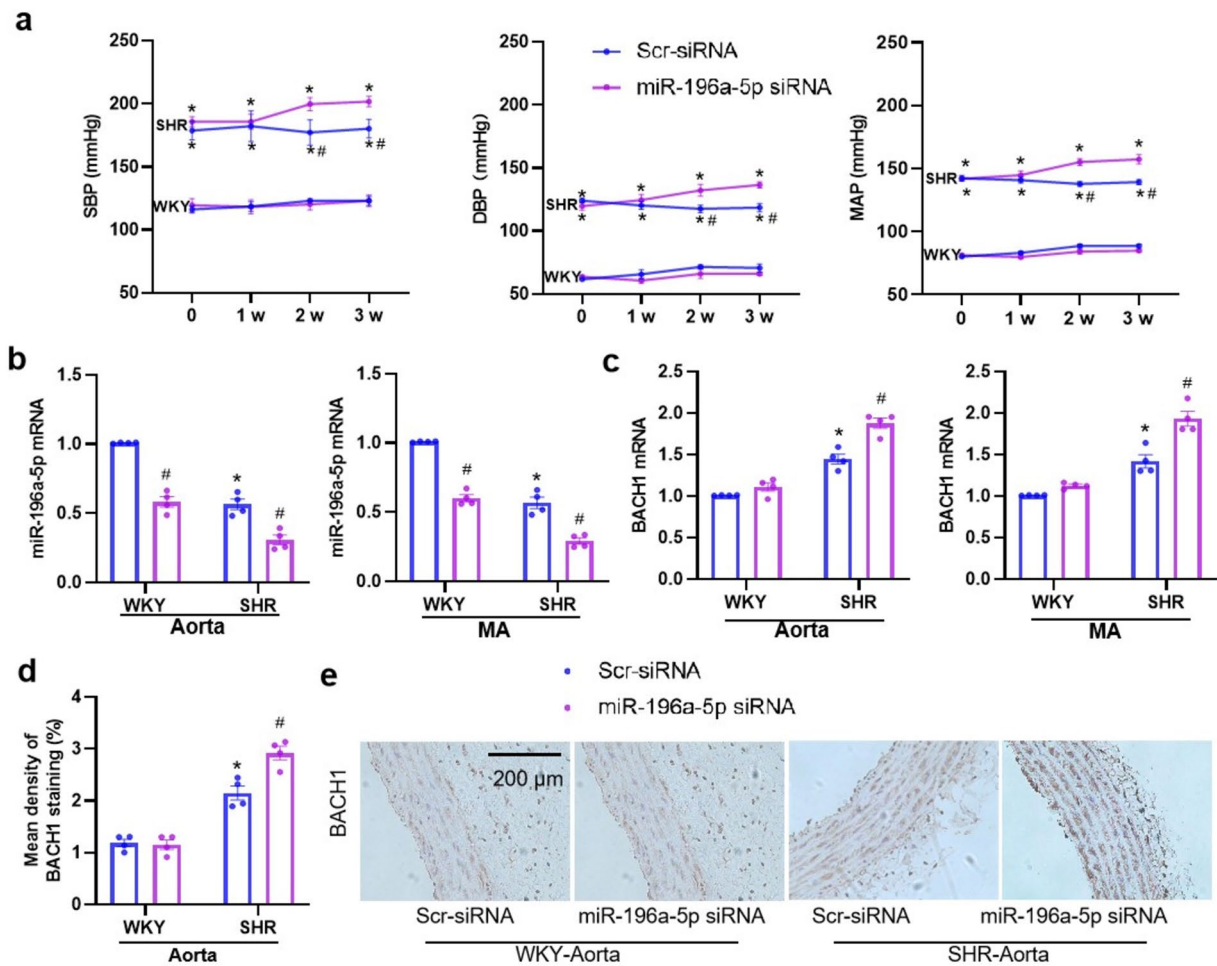


**Figure 7.** Influences of the miR-196a-5p knockdown on blood pressure and BACH1 expression of WKYs and SHRs. The rat was intravenously injected with control lentivirus (Scr-siRNA) or miR-196a-5p-siRNA-lentivirus (miR-196a-5p siRNA,  $2 \times 10^{11}$  plaque forming units/mL, 100  $\mu$ L). (a) Systolic blood pressure (SBP), diastolic blood pressure (DBP), and mean arterial pressure (MAP) were measured once a week in awake state. (b) miR-196a-5p levels in the aortic and MA tissues. (c) BACH1 mRNA levels in aortic and MA tissues. (d) Bar graph showing the relative density of BACH1 staining in aortic tissues. (e) Representative images of immunohistochemistry for BACH1 (brown color) in aortic tissues. Values were denoted as mean  $\pm$  SEM. \*  $p < 0.05$  vs WKY. #  $p < 0.05$  vs Scr-siRNA.  $n = 4$ .

## Materials and methods

### Experimental animals

Male Wistar-Kyoto rats (WKYs) and SHRs were obtained from Vital River Laboratory Animal Technology Co. Ltd (Beijing, China). Male rats aged at 8 weeks were used for isolation of primary VSMCs and male rats aged 10 weeks were used for animal experiments<sup>30</sup>. Animal-involved procedures complied with the Guide for the Care and Use of Laboratory Animals (NIH, 8th edition, 2011), and received approval from the Experimental Animal Care and Use Committee of Nanjing Medical University (IACUC No: 2107007). Animals were housed in a 12-h light/12-h dark cycle with a temperature controlled room. The rats were fed with a standard chow and tap water ad libitum. The rat was euthanized with an overdose of pentobarbital sodium (200 mg/kg, iv) at the end of the experiment.

### Primary culture of VSMCs

Primary rat aortic tissues were sampled for isolation of VSMCs. Briefly, through longitudinal incision was performed to peel off the intima, which was then separated and treated with 0.4% Type 1A collagenase in PBS for digestion for 30 min. The cells were isolated and re-suspended in DMEM mixed with 10% fetal bovine serum, 100 IU/mL penicillin and 10 mg/mL streptomycin maintained in 5% CO<sub>2</sub> at 37 °C.

### Knocking down BACH1 in VSMCs

BACH1-siRNA-lentivirus ( $1 \times 10^9$  TU/mL) were produced by Genaray Biotech Co., Ltd. (Shanghai, China). Sequence of BACH1-siRNA-lentivirus nucleotide was 5'-GGAACCGACAAGATCCGAAGT-3'.

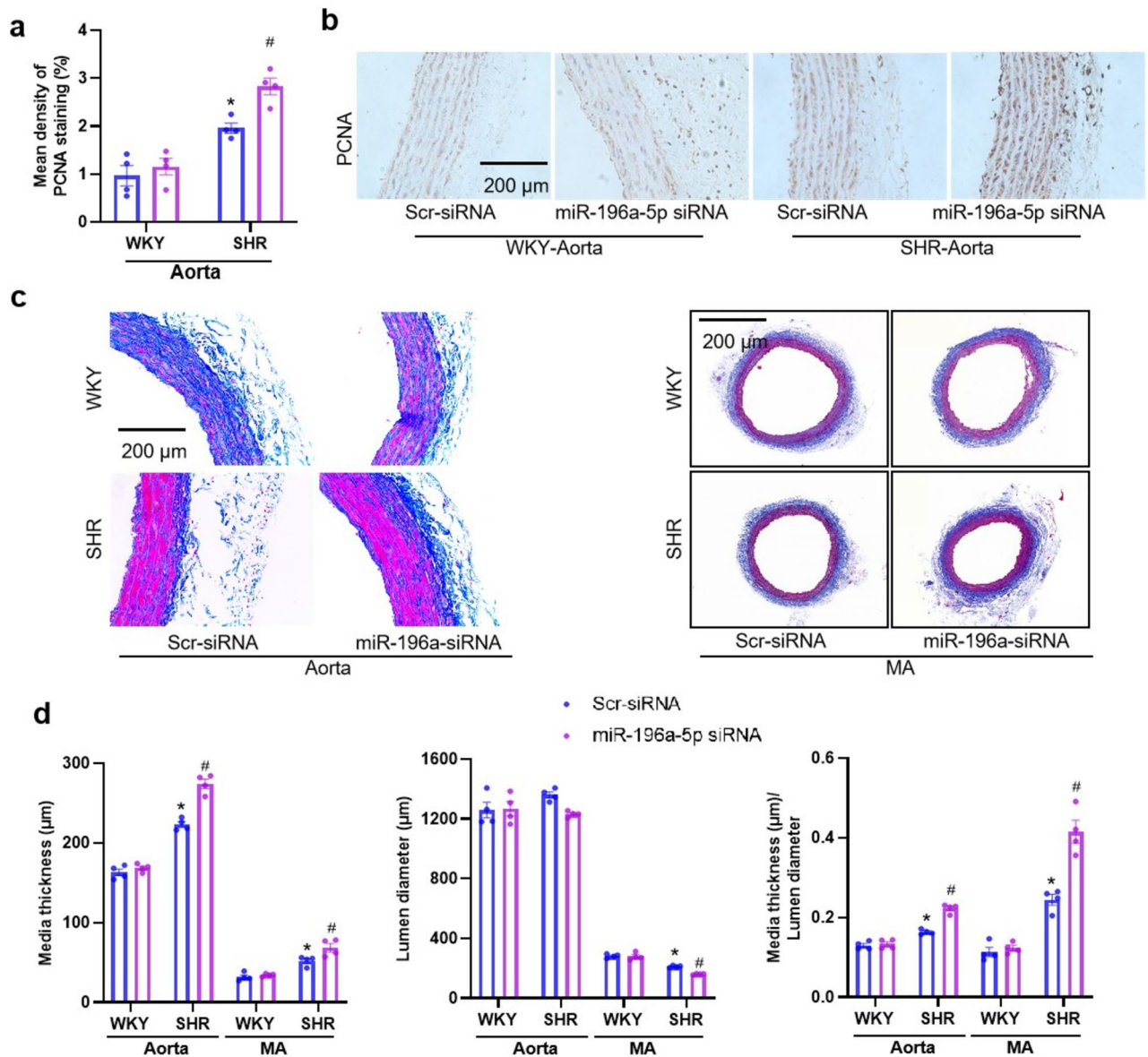


**Figure 8.** Influences of the miR-196a-5p knockdown on vascular remodeling of WKYs and SHRs. The rat was intravenously injected with control lentivirus (Scr-siRNA) or miR-196a-5p-siRNA-lentivirus (miR-196a-5p siRNA,  $2 \times 10^{11}$  plaque forming units/mL, 100  $\mu$ L). (a) Bar graph showing the relative density of PCNA staining in aortic tissues. (b) Representative images of immunohistochemistry for PCNA (brown color) in aortic tissues. (c) Representative images of Masson's staining of aortic and MA tissues. (d) Bar graph showing the Masson's staining analysis for media thickness, lumen diameter and their ratio in aortic and MA tissues. Values were denoted as mean  $\pm$  SEM. \*  $p < 0.05$  vs WKY. #  $p < 0.05$  vs Scr-siRNA.  $n = 4$ .

BACH1-siRNA-lentivirus (MOI = 80) were introduced to infect VSMCs, with scrambled siRNA as negative control. Forty eight hours later, the expression of BACH1 was calculated.

#### Transfection of miR-196a-5p mimics

VSMCs ( $5 \times 10^5$  cells/well) were planted into 6-well plates for 18 h of culture, followed by transfection with 50 nmol/L miR-196a-5p mimics, or 6  $\mu$ L of negative controls containing RNAiFectin™ reagent. The medium was replaced six hours later to eliminate the reagent. The efficiency of transfection was detected after 24 h. All transfection reagents were offered by Applied Biological Materials Inc. (Richmond, BC, Canada).

#### Knocking down miR-196a-5p in VSMCs and rats

Lentiviral vectors, which targeted miR-196a-5p (miR-196a-5p siRNA) and scrambled siRNA (Scr-siRNA), were provided by Genomeditech Co., Ltd (Shanghai, China). Transfection of VSMCs with Scr-siRNA or miR-196a-5p

siRNA (40 MOI) was accomplished in 6-well plates. All WKYs or SHR were intravenously injected with miR-196a-5p siRNA or Scr-siRNA ( $2 \times 10^{11}$  plaque forming units/mL, 100  $\mu$ L).

### VSMC proliferation assay

CCK8 method and EdU incorporation assay were used to evaluate VSMC proliferation. According to the manufacturer's instructions, VSMC proliferation was measured with CCK-8 kits (Beyotime Institute of Biotechnology, Shanghai, China) and then absorbance was detected at 450 nm using a microplate reader (ELX800, BioTek, Vermont, USA). EdU incorporation assay (Cell-Light™ EdU Apollo®567 In Vitro Imaging Kit, Guangzhou Ribio-Bio, Guangzhou, China) was also used to examine VSMC proliferation. EdU-positive cells were counted, and normalized according to total Hoechst 33,342 stained cells.

### DHE assay

Dihydroethidium (DHE) assay was performed to evaluate ROS level in VSMCs. Incubation of VSMCs (about  $3 \times 10^5$  cells/mL) was accomplished in six-well plates with 10  $\mu$ M DHE in the dark and humidity at 37 °C for 30 min, then 40,6-diamidino-2-phenylindole (DAPI) was used to stain cell nuclei for 10 min at room temperature. Having been washed thrice with PBS, fluorescence was examined under excitation at 518 nm and emission at 605 nm with a fluorescence microscope (DP70, Olympus Optical, Tokyo, Japan).

### NAD(P)H oxidase activity assay

NAD(P)H oxidase was determined for activity using a commercial kit (Abcam; Cambridge, MA, USA), with optical density read at 450 nm by a Microplate Reader (STNERGY/H4, BioTek, Vermont, USA).

### Dual luciferase reporter assay

VSMCs were allowed to grow to a confluence 85–90%, followed by co-transfection with 1  $\mu$ g/mL pcDNA-BACH1 reporter plasmids, produced by Genaray Biotech Co., Ltd. (Shanghai, China), and then with normal control and miR-196a-5p mimics (50 nmol/L) by the Lipofectamine™3000 transfection reagent. Luciferase activity was computed using the dual-luciferase reporter assay system.

### Western blot analysis

Sample homogenization in lysis buffer containing 1% PMSF was accompanied by protein extraction with a BCA protein assay kit (BCA; Pierce, Santa Cruz, CA, USA), isolation with sodium dodecyl sulfate–polyacrylamide gel electrophoresis (SDS-PAGE), as well as blotting with a polyvinylidene fluoride (PVDF) membrane. Then, Enhanced Chemiluminescence Detection Kit (Thermo Fisher Scientific, Rockford, IL, USA) was adopted to determine bands of proteins. Antibodies against NOX2 (1:2000, A19701), NOX4 (1:2000, A11274), BACH1 (1:2000, A5393),  $\beta$ -actin (1:2000, AC006) and secondary antibodies (1:10,000, AS014) were purchased from ABclonal (ABclonal Technology Co.,Ltd, Wuhan, China).

### Measurement of miR-196a-5p level

Following total RNA extraction with miRcute miRNA isolation kit were quantification with NanoDrop 2000 Spectrophotometer (Thermo-Fisher Scientific, Wilmington, DE, USA), reverse-transcription to cDNA by the miRcute Plus miRNA First-Strand cDNA kit (Tiangen Biotech). Quantitative Reverse Transcriptase PCR (qRT-PCR) was implemented to determine the expression of miRNA, with U6 small nuclear RNA as an internal control for normalization.

### Immunohistochemistry

The expression levels of BACH1 and PCNA were expressed in the aortic tissues of WKYs and SHR. Primary anti-BACH1 antibodies (1:100) and anti-PCNA antibodies (1:100) were offered by from Abcam and Protein Tech Group Inc. Santa Cruz Biotechnology Inc provided the horseradish peroxidase-conjugated goat anti-rabbit antibody. Positive cells were shown by 3,3-Diaminobenzidine. After counterstaining with hematoxylin, photos were taken by a light microscope (BX-51, Olympus, Tokyo, Japan). ImageJ software (v1.80; NIH, Bethesda, Maryland) was used for quantitative analysis of intensity of density, tissue area measurement and ratio of intensity of density to tissue area<sup>42</sup>.

### Masson's staining

Masson's trichrome staining was used to assess vascular remodeling of aortas and MAs from WKYs and SHR<sup>30</sup>. Photos were made by a light microscope, and quantitation was run on the ImageJ software. Vascular remodeling was assessed according to parameters of media thickness, lumen diameter, ratio of media thicknesses to lumen diameter, outer diameter, and media cross-sectional area.

### Blood pressure measurement

Tail artery blood pressure was measured weekly in conscious WKYs and SHR using a tail-cuff system (NIBP, ADInstruments, Sydney, New South Wales, Australia). The blood pressure values from four measurements were averaged as the result.

### Real-time PCR

Total RNA extraction was performed using Trizol reagent (Life Technologies, Gaithersburg, MD, USA). RNA concentration and purity were determined by the optical density at 260 and 280 nm. Reverse transcriptase

reactions were introduced by the PrimeScript® RT reagent kits (Takara, Otsu, Shiga, Japan) and ABI PRISM 7500 sequence detection PCR system (Applied Biosystems, Foster City, CA, USA). GAPDH small nuclear RNA was used as an internal control for normalization. Primers sequences are listed in the Online-only Data Supplement (Table S1).

### Statistical analysis

Data expressed as mean ± SEM statistical significance was determined by One-way/two-way ANOVA, followed by Bonferroni's post-test, when appropriate. A level at  $p < 0.05$  indicated statistical difference.

### Quality assessment

The quality of the included animal studies was evaluated according to the ARRIVE 2.0 guideline.

### Data availability

The datasets generated during this study are available from the corresponding author on reasonable request.

Received: 25 February 2024; Accepted: 19 July 2024

Published online: 23 July 2024

### References

- Zhang, J. R. *et al.* MiRNAs, lncRNAs, and circular RNAs as mediators in hypertension-related vascular smooth muscle cell dysfunction. *Hypertens. Res.* **44**, 129–146. <https://doi.org/10.1038/s41440-020-00553-6> (2021).
- Shirazi-Tehrani, E. *et al.* ncRNAs and polyphenols: New therapeutic strategies for hypertension. *RNA Biol.* **19**, 575–587. <https://doi.org/10.1080/15476286.2022.2066335> (2022).
- Maguire, E. M. *et al.* Noncoding RNAs in vascular smooth muscle cell function and neointimal hyperplasia. *FEBS J.* **287**, 5260–5283. <https://doi.org/10.1111/febs.15357> (2020).
- Sun, H. J. *et al.* current opinion for hypertension in renal fibrosis. *Adv. Exp. Med. Biol.* **1165**, 37–47. [https://doi.org/10.1007/978-981-13-8871-2\\_3](https://doi.org/10.1007/978-981-13-8871-2_3) (2019).
- Zhang, J. R. *et al.* lncRNAs and circular RNAs as endothelial cell messengers in hypertension: Mechanism insights and therapeutic potential. *Mol. Biol. Rep.* **47**, 5535–5547. <https://doi.org/10.1007/s11033-020-05601-5> (2020).
- Wu, M. *et al.* Circular RNAs: Regulators of vascular smooth muscle cells in cardiovascular diseases. *J Mol Med.* **100**, 519–535. <https://doi.org/10.1007/s00109-022-02186-3> (2022).
- Ma, J. *et al.* Signaling pathways in vascular function and hypertension: Molecular mechanisms and therapeutic interventions. *Signal Transduct. Target Ther.* **8**, 168. <https://doi.org/10.1038/s41392-023-01430-7> (2023).
- Leung, A. *et al.* Functional long non-coding RNAs in vascular smooth muscle cells. *Curr. Top Microbiol. Immunol.* **394**, 127–141. [https://doi.org/10.1007/82\\_2015\\_441](https://doi.org/10.1007/82_2015_441) (2016).
- Hartmann, D. *et al.* MicroRNA-based therapy of GATA2-deficient vascular disease. *Circulation.* **134**, 1973–1990. <https://doi.org/10.1161/circulationaha.116.022478> (2016).
- Gangwar, R. *et al.* Noncoding RNAs in cardiovascular disease: pathological relevance and emerging role as biomarkers and therapeutics. *Am. J. Hypertens.* **31**, 150–165. <https://doi.org/10.1093/ajh/hpx197> (2018).
- Mito, S. *et al.* Myocardial protection against pressure overload in mice lacking Bach1, a transcriptional repressor of heme oxygenase-1. *Hypertension.* **51**, 1570–1577. <https://doi.org/10.1161/hypertensionaha.107.102566> (2008).
- Guo, J. *et al.* BACH1 deficiency prevents neointima formation and maintains the differentiated phenotype of vascular smooth muscle cells by regulating chromatin accessibility. *Nucl. Acids Res.* **51**, 4284–4301. <https://doi.org/10.1093/nar/gkad120> (2023).
- Jia, M. *et al.* Deletion of BACH1 attenuates atherosclerosis by reducing endothelial inflammation. *Circ. Res.* **130**, 1038–1055. <https://doi.org/10.1161/circresaha.121.319540> (2022).
- Watari, Y. *et al.* Ablation of the bach1 gene leads to the suppression of atherosclerosis in bach1 and apolipoprotein E double knockout mice. *Hypertens. Res.* **31**, 783–792. <https://doi.org/10.1291/hyres.31.783> (2008).
- Lopes, R. *et al.* Downregulation of nuclear factor erythroid 2-related factor and associated antioxidant genes contributes to redox-sensitive vascular dysfunction in hypertension. *Hypertension.* **66**, 1240–1250. <https://doi.org/10.1161/hypertensionaha.115.06163> (2015).
- Weber, G. J. *et al.* Hypertension exaggerates renovascular resistance via miR-122-associated stress response in aging. *J. hypertension.* **36**, 2226–2236. <https://doi.org/10.1097/hjh.0000000000001770> (2018).
- Goven, D. *et al.* Altered Nrf2/Keap1-Bach1 equilibrium in pulmonary emphysema. *Thorax.* **63**, 916–924. <https://doi.org/10.1136/thx.2007.091181> (2008).
- Wiel, C. *et al.* BACH1 stabilization by antioxidants stimulates lung cancer metastasis. *Cell.* **178**, 330–345.e322. <https://doi.org/10.1016/j.cell.2019.06.005> (2019).
- Lu, Q. B. *et al.* Chicoric acid prevents PDGF-BB-induced VSMC dedifferentiation, proliferation and migration by suppressing ROS/NFκB/mTOR/P70S6K signaling cascade. *Redox Biol.* **14**, 656–668. <https://doi.org/10.1016/j.redox.2017.11.012> (2018).
- Badran, A. *et al.* Reactive oxygen species: Modulators of phenotypic switch of vascular smooth muscle cells. *Int. J. Mol. Sci.* **21**, 8764. <https://doi.org/10.3390/ijms21228764> (2020).
- Sun, H. *et al.* Salusin-β promotes vascular calcification via nicotinamide adenine dinucleotide phosphate/reactive oxygen species-mediated klotho downregulation. *Antioxid Redox Signal.* **31**, 1352–1370. <https://doi.org/10.1089/ars.2019.7723> (2019).
- Almajdoob, S. *et al.* Resveratrol attenuates hyperproliferation of vascular smooth muscle cells from spontaneously hypertensive rats: Role of ROS and ROS-mediated cell signaling. *Vasc. Pharmacol.* **101**, 48–56. <https://doi.org/10.1016/j.vph.2017.12.064> (2018).
- Lacolley, P. *et al.* Smooth muscle cell and arterial aging: Basic and clinical aspects. *Cardiovasc. Res.* **114**, 513–528. <https://doi.org/10.1093/cvr/cvy009> (2018).
- Thompson, A. A. R. *et al.* Targeting vascular remodeling to treat pulmonary arterial hypertension. *Trends Mol. Med.* **23**, 31–45. <https://doi.org/10.1016/j.molmed.2016.11.005> (2017).
- Zhang, J. R. *et al.* Extracellular vesicle-mediated vascular cell communications in hypertension: Mechanism insights and therapeutic potential of ncRNAs. *Cardiovasc. Drugs Ther.* **36**, 157–172. <https://doi.org/10.1007/s10557-020-07080-z> (2022).
- Kumar, S. *et al.* Role of flow-sensitive microRNAs and long noncoding RNAs in vascular dysfunction and atherosclerosis. *Vascul. Pharmacol.* **114**, 76–92. <https://doi.org/10.1016/j.vph.2018.10.001> (2019).
- Vacante, F. *et al.* The function of miR-143, miR-145 and the MiR-143 host gene in cardiovascular development and disease. *Vascul. Pharmacol.* **112**, 24–30. <https://doi.org/10.1016/j.vph.2018.11.006> (2019).
- Du, X. *et al.* Integrated analysis of miRNA-mRNA interaction network in porcine granulosa cells undergoing oxidative stress. *Oxid. Med. Cell. Longev.* **2019**, 1041583. <https://doi.org/10.1155/2019/1041583> (2019).

29. Engedal, N. *et al.* From oxidative stress damage to pathways, networks, and autophagy via MicroRNAs. *Oxid. Med. Cell. Longev.* **2018**, 4968321. <https://doi.org/10.1155/2018/4968321> (2018).
30. Ren, X. S. *et al.* MiR155-5p in adventitial fibroblasts-derived extracellular vesicles inhibits vascular smooth muscle cell proliferation via suppressing angiotensin-converting enzyme expression. *J. Extracell. Vesicles.* **9**, 1698795. <https://doi.org/10.1080/20013078.2019.1698795> (2020).
31. Ye, C. *et al.* Inhibition of miR-135a-5p attenuates vascular smooth muscle cell proliferation and vascular remodeling in hypertensive rats. *Acta. Pharmacol. Sin.* **42**, 1798–1807. <https://doi.org/10.1038/s41401-020-00608-x> (2021).
32. Tong, Y. *et al.* Extracellular vesicle-mediated miR135a-5p transfer in hypertensive rat contributes to vascular smooth muscle cell proliferation via targeting FNDC5. *Vascul. Pharmacol.* **140**, 106864. <https://doi.org/10.1016/j.vph.2021.106864> (2021).
33. Tong, Y. *et al.* MiR-155-5p attenuates vascular smooth muscle cell oxidative stress and migration via inhibiting BACH1 expression. *Biomedicines.* **11**, 1679. <https://doi.org/10.3390/biomedicines11061679> (2023).
34. Zhou, B. *et al.* MiR-31-5p promotes oxidative stress and vascular smooth muscle cell migration in spontaneously hypertensive rats via inhibiting FNDC5 expression. *Biomedicines.* **9**, 1009. <https://doi.org/10.3390/biomedicines9081009> (2021).
35. de Almeida Oliveira, N. C. *et al.* Multicellular regulation of miR-196a-5p and miR-425-5 from adipose stem cell-derived exosomes and cardiac repair. *Clin. Sci.* **136**(17), 1281–1301. <https://doi.org/10.1042/cs20220216> (2022).
36. Tan, L. *et al.* Identification of key genes and pathways affected in epicardial adipose tissue from patients with coronary artery disease by integrated bioinformatics analysis. *Peer J.* **8**, e8763. <https://doi.org/10.7717/peerj.8763> (2020).
37. NandyMazumdar, M. *et al.* BACH1, the master regulator of oxidative stress, has a dual effect on CFTR expression. *Biochem J.* **478**, 3741–3756. <https://doi.org/10.1042/bcj20210252> (2021).
38. Nishizawa, H. *et al.* Ferroptosis: Regulation by competition between NRF2 and BACH1 and propagation of the death signal. *FEBS J.* **7**, 1688–1704. <https://doi.org/10.1111/febs.16382> (2022).
39. Sun, J. *et al.* Hemoprotein Bach1 regulates enhancer availability of heme oxygenase-1 gene. *EMBO J.* **21**, 5216–5224. <https://doi.org/10.1093/emboj/cdf516> (2002).
40. Igarashi, K. *et al.* The transcription factor BACH1 at the crossroads of cancer biology: From epithelial-mesenchymal transition to ferroptosis. *J Biol Chem.* **297**, 101032. <https://doi.org/10.1016/j.jbc.2021.101032> (2021).
41. Zhang, X. *et al.* Bach1: Function, regulation, and involvement in disease. *Oxid Med Cell Longev.* **2018**, 1347969. <https://doi.org/10.1155/2018/1347969> (2018).
42. Zheng, M. *et al.* Hippo–Yap signaling maintains sinoatrial node homeostasis. *Circulation.* **146**, 1694–1711. <https://doi.org/10.1161/CIRCULATIONAHA.121.058777> (2022).

### Author contributions

YT, DDW, YLZ, SH, and QFP designed experiments. YT, DDW, YLZ, SH, DC, and YXW conducted the experiments. YT, DDW, YLZ, SH, DC, YXW, and QFP performed data and statistical analyses. YT, DDW, and QFP wrote the manuscript, with contributions from all the other authors. QFP supervised the study. All authors reviewed the manuscript approved the final version for submission.

### Funding

This study was supported by the National Natural Science Foundation of China (82200475); Natural Science Foundation of Jiangsu Province (BK20221087).

### Competing interests

The authors declare no competing interests.

### Additional information

**Supplementary Information** The online version contains supplementary material available at <https://doi.org/10.1038/s41598-024-68122-2>.

**Correspondence** and requests for materials should be addressed to Q.-F.P.

**Reprints and permissions information** is available at [www.nature.com/reprints](http://www.nature.com/reprints).

**Publisher's note** Springer Nature remains neutral with regard to jurisdictional claims in published maps and institutional affiliations.



**Open Access** This article is licensed under a Creative Commons Attribution-NonCommercial-NoDerivatives 4.0 International License, which permits any non-commercial use, sharing, distribution and reproduction in any medium or format, as long as you give appropriate credit to the original author(s) and the source, provide a link to the Creative Commons licence, and indicate if you modified the licensed material. You do not have permission under this licence to share adapted material derived from this article or parts of it. The images or other third party material in this article are included in the article's Creative Commons licence, unless indicated otherwise in a credit line to the material. If material is not included in the article's Creative Commons licence and your intended use is not permitted by statutory regulation or exceeds the permitted use, you will need to obtain permission directly from the copyright holder. To view a copy of this licence, visit <http://creativecommons.org/licenses/by-nc-nd/4.0/>.

© The Author(s) 2024